

## Atmospheric response to observed intraseasonal tropical sea surface temperature anomalies

Adrian J. Matthews

School of Environmental Sciences and School of Mathematics, University of East Anglia, Norwich, UK

Received 7 May 2004; revised 10 June 2004; accepted 24 June 2004; published 27 July 2004.

[1] The major tropical convective and circulation features of the intraseasonal or Madden–Julian oscillation (MJO) are simulated as a passive response to observed MJO sea surface temperature (SST) anomalies in an atmospheric general circulation model (AGCM), strengthening the case for ocean–atmosphere interactions being central to MJO dynamics. However, the magnitude of the surface fluxes diagnosed from the MJO cycle in the AGCM, that would feed back onto the ocean in a coupled system, are much weaker than in observations. The phasing of the convective–dynamical model response to the MJO SST anomalies and the associated surface flux anomalies is too fast compared to observations of the (potentially) coupled system, and would act to damp the SST anomalies. *INDEX TERMS:* 1620 Global Change: Climate dynamics (3309); 3339 Meteorology and Atmospheric Dynamics: Ocean/atmosphere interactions (0312, 4504); 3374 Meteorology and Atmospheric Dynamics: Tropical meteorology; 9340 Information Related to Geographic Region: Indian Ocean; 9355 Information Related to Geographic Region: Pacific Ocean. **Citation:** Matthews, A. J. (2004), Atmospheric response to observed intraseasonal tropical sea surface temperature anomalies, *Geophys. Res. Lett.*, *31*, L14107, doi:10.1029/2004GL020474.

### 1. Introduction

[2] The Madden–Julian oscillation (MJO) is the dominant mode of atmospheric tropical variability on intraseasonal time scales. It is characterized by large-scale convective anomalies that develop over the tropical Indian Ocean and propagate slowly eastward over the maritime continent to the western Pacific [Madden and Julian, 1972]. Individual MJO events last typically between 30 and 60 days. Large-scale pressure and circulation anomalies develop with the convective anomalies and can be interpreted as a moist equatorial Kelvin–Rossby wave response in the tropics [Hendon and Salby, 1994; Matthews, 2000].

[3] Recently, the importance of ocean–atmosphere interactions within the MJO have been emphasized. Positive (negative) sea surface temperature (SST) anomalies lead the enhanced (suppressed) MJO convection by approximately 10–12 days (a quarter cycle), consistent with the atmosphere responding to the ocean forcing [Sperber *et al.*, 1997; Shinoda *et al.*, 1998; Woolnough *et al.*, 2000]. The SST anomalies themselves have been simulated in thermodynamical ocean models as the response to the observed anomalous surface fluxes of latent heat and shortwave radiation [Shinoda and Hendon, 1998] without the need to

invoke ocean dynamics. Coupling an ocean model to an atmospheric model has improved the simulation of the MJO from that in the atmospheric model alone in some cases [Flatau *et al.*, 1997; Waliser *et al.*, 1999; Inness and Slingo, 2003] but has had no beneficial effect in others [Hendon, 2000]. Such improvement appears to be dependent on an accurate simulation of the mean climate and a correct representation of the surface fluxes [Inness *et al.*, 2003; Hendon, 2000]. This is particularly true of the latent heat flux, which is proportional to the *total* surface wind speed, i.e., the magnitude of the sum of the climatological mean and anomalous wind vectors.

[4] The atmospheric response to tropical intraseasonal SST anomalies has been addressed by Woolnough *et al.* [2001], who examined the equilibrium response to an idealized, eastward-propagating equatorial SST dipole anomaly in an “aquaplanet” atmospheric general circulation model (AGCM). When the eastward phase speed of the imposed SST anomaly was similar to that of the MJO (approximately  $5 \text{ m s}^{-1}$ ), there was a significant atmospheric response, with a region of enhanced convection lagging (lying to the west of) the positive SST anomaly, consistent with observations of the MJO. However, the implied feedback onto the ocean by this atmospheric response could not be diagnosed, as the climatological mean tropical surface winds were easterly throughout the tropics in this aquaplanet simulation and, therefore, the latent heat flux with its dependence on the *total* surface wind could not be expected to be realistic.

### 2. Model

[5] This study extends the previous work on the role of the ocean in the MJO by examining the atmospheric response to realistic observed MJO SST anomalies in a full AGCM with an accurate climatological mean state, such that the implied feedback onto the ocean can be diagnosed. The AGCM used was the UK Met Office Unified Model (HadAM3), the aquaplanet version of which was used by Woolnough *et al.* [2001]. The model had a spatial resolution of  $3.75^\circ$  longitude  $\times$   $2.5^\circ$  latitude and 30 vertical levels. The deep convective parameterization scheme was based on a mass flux approach and closed on buoyancy. For further details, see Pope *et al.* [2000]. The amount of tropical intraseasonal variability simulated by the Unified Model AGCM has been shown to be realistic [Slingo *et al.*, 1996], but on close inspection the eastward propagation of intraseasonal convective anomalies was rather incoherent [Matthews *et al.*, 1999; Inness *et al.*, 2001], albeit in an earlier version of the model. When the AGCM was coupled to an ocean GCM, the simulation of the MJO improved,

especially over the Indian Ocean [Inness and Slingo, 2003]. However, the coupled GCM (HadCM3) suffered from a mean equatorial cold tongue bias and associated atmospheric circulation errors over the western Pacific, such that the model MJO did not propagate further eastward than Indonesia. When a flux correction was applied to rectify this, the MJO propagated out into the western Pacific [Inness *et al.*, 2003].

[6] Here, the AGCM was forced with global observed SSTs for the 21 year period from 1 January 1982 to 31 December 2002. The SSTs were taken from the optimally interpolated Reynolds SST data set [Reynolds *et al.*, 2002]. The data were available on a  $1^\circ \times 1^\circ$  grid as weekly means, which is a sufficient resolution to resolve MJO fluctuations. They were spatially averaged onto the coarser AGCM grid, and then temporally interpolated to daily values for ease of computation. The MJO in both the observations and the model was then defined purely on the basis of its SST component. This enabled a direct comparison to be made between the observations and the model, as the SST fields were the same for both. First, the annual cycle (mean and first three annual harmonics) of the SST were subtracted at each grid point. Then the data were passed through a 20–200-day band pass Lanczos filter with 241 weights to isolate the intraseasonal variability. An empirical orthogonal function (EOF) analysis was then applied to the filtered SST data over the tropical warm pool region ( $40^\circ\text{E}$ – $170^\circ\text{W}$ ,  $20^\circ\text{S}$ – $10^\circ\text{N}$ ) to find the dominant modes of variability. The first two EOFs were significant and explained 11% and 9% of the variance, respectively. Together with their principal component time series, they described eastward-propagating SST anomalies with an average time period of approximately 48 days, i.e., the MJO. A composite MJO life cycle was then defined by assigning each day to a phase of the MJO, depending on the amplitude of the first two EOFs. Only data from the northern winter season (November–April) were included, as the MJO is most coherent then. Full details of this technique are described by Hall *et al.* [2001].

### 3. MJO Cycle

[7] The observed MJO, as defined by the analysis of SST, is summarized in a Hovmöller diagram (Figure 1a). On day 0 of the MJO cycle, positive SST anomalies are located over the tropical Indian Ocean. These propagate eastward into the western Pacific by day 24, and are followed in the second half of the cycle by the eastward propagation of a negative SST anomaly. Outgoing longwave radiation (OLR) was used as a proxy for deep tropical convection. The data were available as daily maps on a  $2.5^\circ \times 2.5^\circ$  grid [Liebmann and Smith, 1996]. Enhanced deep convection (negative OLR anomalies) lag the positive SST anomalies temporally by 12 days (a quarter cycle) and spatially by approximately  $30^\circ$  longitude to the west. Suppressed convection then follows the cool SSTs. This behavior is consistent with previous studies based on OLR [e.g., Shinoda and Hendon, 1998], although the OLR amplitude here is approximately half that in such studies, presumably due to the component of the MJO that is independent of SST, and to sampling variability. Hence, the analysis based on SST presented here does capture the main features of the MJO.

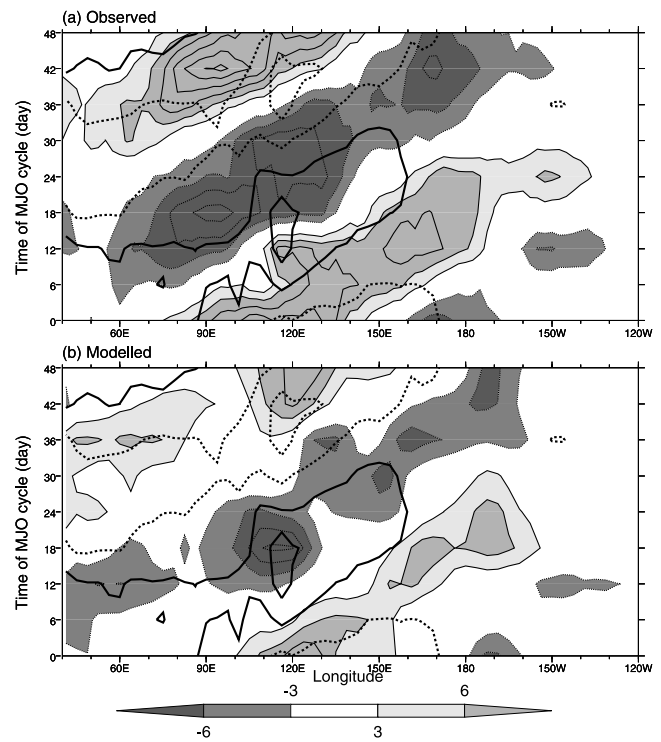


**Figure 1.** Time-longitude diagram of anomalous equatorial SST and OLR (averaged  $15^\circ\text{S}$ – $5^\circ\text{N}$ ). (a) Observed, (b) modelled. SST anomalies are contoured heavily. The contour interval is  $0.2^\circ\text{C}$ ; the first positive contour is at  $0.1^\circ\text{C}$ . Negative contours are dotted and the zero contour is suppressed. OLR contour interval is  $3 \text{ W m}^{-2}$ ; see legend for shading. See color version of this figure in the HTML.

[8] The SST cycle in the model (Figure 1b) is identical to the observations by design. The convective response to the MJO SST forcing is broadly similar to that in the observed MJO. Negative (positive) OLR anomalies propagate eastward and lag the positive (negative) SST anomalies, although the amplitude is slightly weaker than in the observations, and convection lags the SST by only 4 days, compared to 12 days (a quarter cycle) in the observations. It should be emphasized that the model MJO shown here is *purely* the passive atmospheric response to the imposed MJO SST anomalies. Any intrinsic atmospheric-only MJO variability in the model that is independent of the ocean will not be picked up by this analysis. Hence, atmospheric convection *can* respond significantly and coherently on intraseasonal time scales to realistic MJO SST anomalies. On the other hand, the observed MJO (Figure 1a) potentially has components of variability that are fully coupled or just one-way interactions with the ocean forcing the atmosphere or vice versa. Hence, the modelled and observed MJO cycles shown here would not be expected to be identical.

[9] The spatial structure of the observed SST and OLR anomalies for day 0 of the MJO cycle are shown in Figure 2a. The suppressed convection (positive OLR anomalies) over Indonesia lies to the west of the negative SST anomalies in the western Pacific. There is enhanced convection over the western Pacific and along the South Pacific Convergence Zone. The observed near-surface ( $1000\text{-hPa}$ ) wind anomalies, from the National Centers for

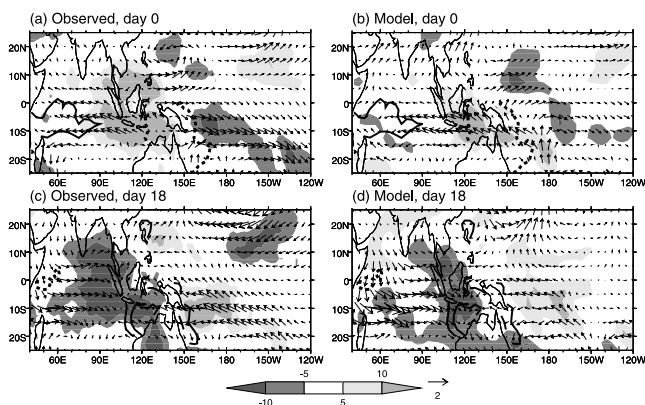


**Figure 2.** Composite maps of SST, OLR and 1000-hPa vector wind anomalies on day 0 for (a) observed and (b) modelled fields, and on day 18 for (c) observed and (d) modelled fields. SST is contoured heavily; interval is 0.2°C, negative contours are dotted and the zero contour is suppressed. OLR anomalies are shaded darkly below  $-5 \text{ W m}^{-2}$  and lightly above  $5 \text{ W m}^{-2}$  (see legend). The standard wind vector has magnitude  $2 \text{ m s}^{-1}$ . See color version of this figure in the HTML.

Environmental Prediction–National Center for Atmospheric Research reanalysis [Kalnay *et al.*, 1996], can be interpreted as an equatorial Rossby–Kelvin wave response to the convective dipole anomaly. There are equatorial easterly anomalies and off-equatorial anticyclonic circulation over the Indian Ocean to the west of the suppressed convection and anomalous equatorial westerly flow and off-equatorial cyclonic circulation over the western Pacific to the east of the suppressed convection and collocated with the enhanced convection. The model convective and dynamical response to the imposed MJO SST anomalies on day 0 of the cycle (Figure 2b) simulates the main observed features, particularly the equatorial easterly and westerly anomalies. However, the region of suppressed convection over Indonesia in the model is located further eastward in the model compared to the observations.

[10] After 18 days, the positive SST anomaly has moved eastward to Indonesia, and a large region of enhanced convection, together with equatorial westerly and off-equatorial cyclonic anomalous flow has developed to the west of this over the Indian Ocean in the observations, while there is suppressed convection over the western Pacific (Figure 2c). The model response to the SST anomalies again broadly reproduces the observed features (Figure 2d), although the convective response is again located further eastward than in the observations.

#### 4. Surface Fluxes

[11] Given that the model response to the imposed MJO SST anomalies is realistic, it is informative to examine the surface flux anomalies in the model through the MJO cycle. If an interactive ocean model was coupled to the AGCM, these fluxes would then feed back onto the ocean. The shortwave flux is defined as positive downwards, and the latent heat flux is defined as positive upwards, according to the usual convention. The surface shortwave flux anomalies (Figure 3a) mirror the deep convective response (Figure 1b)

as the clouds reflect and absorb incoming solar radiation, reducing the surface flux. In common with the deep convection, the reduction in shortwave radiation in the model (i.e., an ocean cooling tendency) follows the positive SST anomalies by only 4 days, compared to 10–12 days (a quarter cycle) in observations [Shinoda *et al.*, 1998; Woolnough *et al.*, 2000; Sperber, 2003].

[12] The model latent heat flux anomalies (Figure 3b) are mainly due to the changes in surface wind speed (Figures 2b and 2d). Positive latent heat flux anomalies, which would lead to an ocean cooling, lag the positive SST anomalies by a similar 4 day interval to the shortwave flux. This is in contrast to the observed MJO, where enhanced evaporation leads the negative SST anomaly phase by approximately 6–8 days, or alternatively lags the positive SST anomaly by about 18 days [Shinoda *et al.*, 1998; Woolnough *et al.*, 2000]. The amplitude of both the shortwave and latent heat flux anomalies in the model is of order  $5 \text{ W m}^{-2}$ , which is a factor of 3–4 weaker than in the observations.

#### 5. Conclusions

[13] An AGCM reproduced the main features of the MJO as a passive response to forcing by observed SST fields at weekly resolution. Coherent, large-scale tropical convective anomalies propagated eastward, lagging the tropical SST anomalies. The dynamical response to these convective anomalies included a realistic equatorial Rossby–Kelvin wave signal in the tropics. We have shown here that observed MJO SST anomalies can force a realistic atmospheric MJO. Given that previous studies have shown that

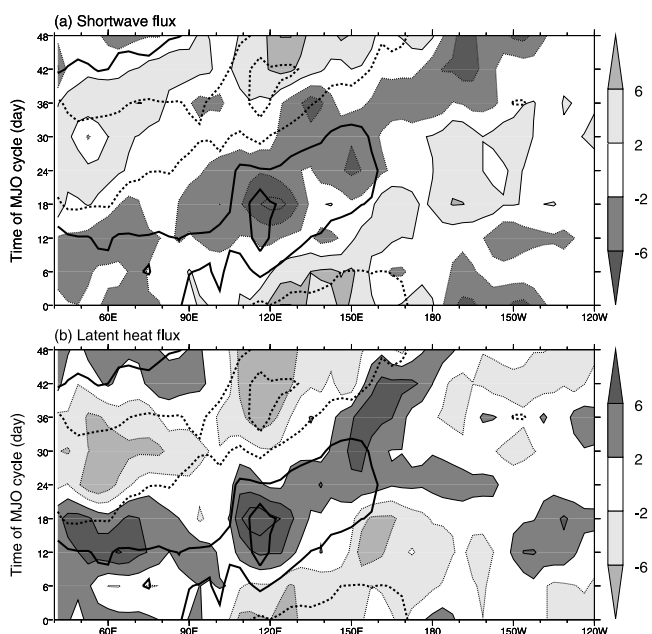


**Figure 3.** Time-longitude diagram of anomalous equatorial SST and modelled surface (a) latent and (b) shortwave fluxes (averaged 15°S–5°N). SST anomalies are contoured heavily. The contour interval is 0.2°C; the first positive contour is at 0.1°C. Negative contours are dotted and the zero contour is suppressed. The surface flux contour interval is  $4 \text{ W m}^{-2}$ ; the first positive contour is at  $2 \text{ W m}^{-2}$ ; see legend for shading. See color version of this figure in the HTML.

observed MJO flux anomalies can force a realistic ocean MJO SST cycle and that coupling generally improves MJO simulations, the case for the MJO as a coupled ocean–atmosphere phenomenon has been strengthened further.

[14] However, the surface shortwave flux anomalies due to changes in the cloud field and latent heat flux anomalies due to changes in the surface wind field were weaker than in the observations, and there are phase differences between the observed MJO and the MJO modelled as a passive response to imposed SST forcing. The convective response in the model appears to be too fast. This leads to a dynamical response that appears earlier in the cycle, relative to the SST anomalies, in the model than in the observations. The subsequent surface shortwave and latent heat flux anomalies then also appear too early in the cycle. If they were then allowed to feed back onto the ocean, they would erode the original SST anomalies too quickly. These factors could be due to inadequacies in the model parametrizations and the model not being responsive enough to SST anomalies. However, if ocean–atmosphere coupling was introduced, it is possible that an altered phase relationship between the oceanic and atmospheric components of the MJO would emerge [Fu and Wang, 2004]. Future work will address these phasing differences by further analysis of the MJO in a coupled model framework.

[15] **Acknowledgments.** I thank Harry Hendon, Dave Stevens and an anonymous reviewer for comments on the manuscript. The OLR, SST and NCEP–NCAR reanalysis data were provided through the NOAA Climate Diagnostics Center (<http://www.cdc.noaa.gov>).

## References

- Flatau, M., et al. (1997), The feedback between equatorial convection and local radiative and evaporative processes: The implications for intraseasonal oscillations, *J. Atmos. Sci.*, *54*, 2373–2386.
- Fu, X. H., and B. Wang (2004), Differences of boreal summer intraseasonal oscillations simulated in an atmosphere–ocean coupled model and an atmosphere-only model, *J. Clim.*, *17*, 1263–1271.
- Hall, J. D., et al. (2001), The modulation of tropical cyclone activity in the Australian region by the Madden-Julian oscillation, *Mon. Weather Rev.*, *129*, 2970–2982.
- Hendon, H. H. (2000), Impact of air–sea coupling on the Madden-Julian oscillation in a general circulation model, *J. Atmos. Sci.*, *57*, 3939–3952.
- Hendon, H. H., and M. L. Salby (1994), The life cycle of the Madden-Julian oscillation, *J. Atmos. Sci.*, *51*, 2225–2237.
- Inness, P. M., and J. M. Slingo (2003), Simulation of the Madden-Julian oscillation in a coupled general circulation model. Part I: Comparison with observations and an atmosphere-only GCM, *J. Clim.*, *16*, 345–364.
- Inness, P. M., et al. (2001), Organization of tropical convection in a GCM with varying vertical resolution: Implications for the simulation of the Madden-Julian oscillation, *Clim. Dyn.*, *17*, 777–793.
- Inness, P. M., et al. (2003), Simulation of the Madden-Julian oscillation in a coupled general circulation model II: The role of the basic state, *J. Clim.*, *16*, 365–382.
- Kalnay, E., et al. (1996), The NCEP/NCAR 40-year reanalysis project, *Bull. Am. Meteorol. Soc.*, *77*, 437–471.
- Liebmann, B., and C. A. Smith (1996), Description of a complete (interpolated) OLR dataset, *Bull. Am. Meteorol. Soc.*, *77*, 1275–1277.
- Madden, R. A., and P. R. Julian (1972), Description of global scale circulation cells in the tropics with a 40–50 day period, *J. Atmos. Sci.*, *29*, 1109–1123.
- Matthews, A. J. (2000), Propagation mechanisms for the Madden-Julian oscillation, *Q. J. R. Meteorol. Soc.*, *126*, 2637–2652.
- Matthews, A. J., et al. (1999), Fast and slow Kelvin waves in the Madden-Julian oscillation of a GCM, *Q. J. R. Meteorol. Soc.*, *125*, 1473–1498.
- Pope, V. D., et al. (2000), The impact of new physical parameterizations in the Hadley Centre climate model: HadAM3, *Clim. Dyn.*, *16*, 123–146.
- Reynolds, R. W., et al. (2002), An improved in situ and satellite SST analysis for climate, *J. Clim.*, *15*, 1609–1625.
- Shinoda, T., and H. H. Hendon (1998), Mixed layer modeling of intraseasonal variability in the tropical Pacific and Indian Oceans, *J. Clim.*, *11*, 2668–2685.
- Shinoda, T., et al. (1998), Intraseasonal variability of surface fluxes and sea surface temperature in the tropical western Pacific and Indian Oceans, *J. Clim.*, *11*, 1685–1702.
- Slingo, J. M., et al. (1996), Intraseasonal oscillations in 15 atmospheric general circulation models: Results from an AMIP diagnostic subproject, *Clim. Dyn.*, *12*, 325–358.
- Sperber, K. R. (2003), Propagation and the vertical structure of the Madden-Julian oscillation, *Mon. Weather Rev.*, *131*, 3018–3037.
- Sperber, K. R., et al. (1997), On the maintenance and initiation of the intraseasonal oscillation in the NCEP/NCAR reanalysis and the GLA and UKMO AMIP simulations, *Clim. Dyn.*, *13*, 769–795.
- Waliser, D. E., et al. (1999), The influence of coupled sea surface temperatures on the Madden-Julian Oscillation: A model perturbation experiment, *J. Atmos. Sci.*, *56*, 333–358.
- Woolnough, S. J., et al. (2000), The relationship between convection and sea surface temperature on intraseasonal timescales, *J. Clim.*, *13*, 2086–2104.
- Woolnough, S. J., et al. (2001), The organisation of tropical convection by intraseasonal sea surface temperature anomalies, *Q. J. R. Meteorol. Soc.*, *127*, 887–907.

A. J. Matthews, School of Environmental Sciences, University of East Anglia, Norwich NR4 7TJ, UK. ([a.j.matthews@uea.ac.uk](mailto:a.j.matthews@uea.ac.uk))